Title

Rod and cone function in coneless mice

Journal

Visual Neuroscience, 22(6)

ISSN

0952-5238

Authors

Williams, G A
Daigle, K A
Jacobs, G H

Publication Date

2005-11-01

Peer reviewed

Visual Neuroscience (2005), **22**, 807–816. Printed in the USA.

DOI: 10.1017/S095252380522610X

Rod and cone function in coneless mice

GARY A. WILLIAMS, KRISTIN A. DAIGLE, AND GERALD H. JACOBS

Neuroscience Research Institute and Department of Psychology, University of California, Santa Barbara, California

(RECEIVED April 18, 2005; ACCEPTED July 7, 2005)

Abstract

Transgenic coneless mice were initially developed to study retinal function in the absence of cones. In coneless mice created by expressing an attenuated diphtheria toxin under the control of flanking sequences from the human L-cone opsin gene, a small number of cones (3–5% of the normal complement) survive in a retina that otherwise appears structurally quite normal. These cones predominantly (~87% of the total) contain UV-sensitive photopigment. ERG recordings, photoreceptor labeling, and behavioral measurements were conducted on coneless and wild-type mice to better understand how the nature of this alteration in receptor complement impacts vision. Signals from the small residual population of UV cones are readily detected in the flicker ERG where they yield signal amplitudes at saturation that are roughly proportional to the number of surviving cones. Behavioral measurements show that rod-based vision in coneless mice does not differ significantly from that of wild-type mice, nor does their rod system show any evidence of age-related deterioration. Coneless mice are able to make accurate rod-based visual discriminations at light levels well in excess of those required to reach cone threshold in wild-type mice.

Keywords: Coneless mice, Ultraviolet-sensitive cones, Photoreceptor labeling, Electroretinogram, Behavioral measurements of visual sensitivity

Introduction

All mammalian retinas contain a mixture of rods and cones and the relative contributions these two receptor types make to vision have been targets of study for upwards of 150 years (Saugstad & Saugstad, 1959; Jacobs, 1993). Rods are more sensitive and allow vision under low light conditions while cones become operative at higher light levels, typically subserving superior temporal and spatial resolution and providing signals required to support color vision. Difficulties in parsing the roles of the two receptor types include the facts that rods and cones share a common interval of functioning, for example covering some four $\log_{10}$ units of light levels in humans (Buck, 2004), and that signals from them share neural pathways in the retina and in the central visual system (Sterling, 2004). To deal with these problems a range of strategies have been developed to separate rod and cone function. These include manipulations of spatial, temporal, and spectral properties of stimulus lights as well as many physiological and pharmacological interventions that were designed to separately access aspects of rod or cone function.

A conceptually different approach to separating rod and cone function involves the study of individuals in whom rod or cone function has been differentially impacted by retinal disease, often traceable to a genetic defect. Examinations of human rod and cone monochromats are well-known examples of this strategy (Alpern et al., 1971; Hess et al., 1987) as are those experiments that exploit gene mutations in experimental animals; for example, a widely studied mouse mutant (rd/rd) shows profound rod degeneration (Carter-Dawson et al., 1978). With the advent of genetic engineering, it additionally became possible to produce experimental animals whose receptor complements have been altered in specific ways. Intriguing examples of the latter are mice of the type that were target of this investigation, so-called coneless mice. A number of different techniques have been used to generate such animals (Soucy et al., 1998; Biel et al., 1999; Ying et al., 2000; Xu et al., 2000). The coneless mouse examined here is a transgenic animal that incorporates a DNA segment encoding the A-chain of an attenuated diphtheria toxin under the control of 6.5 kb of 5′ flanking sequences derived from the human L (long-wavelength sensitive)-cone opsin gene (Soucy et al., 1998). The retinas of these coneless mice appear structurally quite normal with the exception of a profound loss of cone photoreceptors. Further, ganglion cell signals in the coneless mouse derived from rod inputs appeared indistinguishable from those of normal control animals while, at the same time, no ganglion cell signals could be recorded from coneless mice at stimulus light levels where the normal mouse visual system transmits cone-based information (Soucy et al., 1998). Despite their descriptive name, immunocytochemical labeling reveals that a very small fraction (~3–5%) of cones survive in the retinas of coneless mice (Soucy et al., 1998; Raven & Reese, 2003). Like most mammals, mice have two classes of cone, in their case ultraviolet (UV) and middle wavelength (M)

Address correspondence and reprint requests to: Gerald H. Jacobs, Neuroscience Research Institute, University of California, Santa Barbara CA 93106, USA. E-mail: jacobs@psych.ucsb.edu

sensitive (Jacobs et al., 1991), and opsin immunolabeling further shows that virtually all of the surviving cones in the coneless mouse contain UV pigment. It has been suggested that survival of a small number of cones containing UV pigment might reflect variegated expression of the diphtheria toxin gene, perhaps resulting from the fact that the human L-cone opsin gene promoter activity is lower in UV cones than in M cones (Soucy et al., 1998). The (near) absence of cone photoreceptors combined with the apparent normality of the rest of the retina has made the coneless mouse an attractive animal in which to examine a number of hypotheses about the relative roles of rods and cones, their interactions, and their functional consequences (Lucas et al., 1999; Raven & Reese, 2003; Sokal et al., 2003; Dang et al., 2004; Reese et al., 2005).

One focus of our investigation was on the small population of cones that evades ablation in the coneless mouse, specifically asking whether those residual cones contribute signals that have physiological significance. An earlier investigation of coneless mice would seem to suggest that they do not (Soucy et al., 1998). However, that study employed a computer monitor to produce test lights in an attempt to drive ganglion cell responses. Such sources provide only meager energy from the part of spectrum to which the mouse UV photopigment offers significant sensitivity (Jacobs et al., 1991; Lyubarsky et al., 1999) and, thus, signals from a reduced number of photoreceptors might well have escaped detection. We also examined behavioral measurements of visual sensitivity in normal and coneless mice to see how the altered receptor complement of the coneless mouse impacts vision.

Materials and methods

Animals

Coneless transgenic mice were obtained from a breeding colony maintained at the University of California, Santa Barbara (UCSB). These transgenic mice were initially produced as described above (and more fully in Soucy et al., 1998) and subsequently mated with C57BL/6 mice to generate mixed litters of wild-type and coneless offspring. Animals were kept on a 12-h dark/12-h light cycle, the latter having an ambient illuminance of 20 lux. Mice that were subjects in behavioral tests were deprived of food for 22 h prior to each daily test session. These animals were routinely weighed and then fed in an amount sufficient to keep them at not less than 90% of their free-feeding weight. All of the procedures were conducted under protocols approved by the Institutional Animal Care and Use Committee at UCSB. Three types of observations were made on both coneless and wild-type (littermate) mice, the latter serving as control animals.

Electroretinogram (ERG) recording

ERGs were recorded using equipment and procedures described earlier (Jacobs et al., 1996, 2004). Mice were anesthetized with an IM injection of a mixture of xylazine hydrochloride (8 mg/kg) and ketamine hydrochloride (42 mg/kg). The pupil was dilated by topical application of atropine sulfate (0.04%). During the recording session normal body temperature was maintained with a circulating hot-water heading pad. Animals were placed in a head restraint and aligned with an optical system so that stimulus lights could be imaged on the retina in Maxwellian view (59 deg, circular spot). ERGs were differentially recorded from a pair of stainless-steel ring electrodes concentrically placed against the cornea and the conjunctiva (Jacobs et al., 1999). Stimulus lights were derived from a three-beam optical system in which the lights from the three sources are optically superimposed. Test lights came from a monochromator (15 nm half-energy passband) equipped with a 150-W xenon lamp; their intensities were controlled with a circular 3.0 log unit neutral-density wedge. Lights from the other two beams were used for reference and adaptation purposes; these originated from 50-W tungsten-halide sources and their content was modulated with step filters. Stimulus intensities were measured in the plane of the pupil using a calibrated photodiode (PIN 10 DF, United Detector Technology, Hawthorne, CA). Wavelength calibrations were made with an Ocean Optics Spectrometer (USB 2000 UV-VIS).

The stimuli were light pulses flickered at 12.5 Hz (25% duty cycle) and presented in a train of 70 pulses. The fundamental response component to the last 50 of these was extracted by filtering and averaged. Three sets of ERG measurements were made. First, we attempted to phenotype coneless mice by recording ERGs elicited by an achromatic light (2850 K, 2.7 log td) and by a 390-nm monochromatic light. Second, spectral sensitivity measurements were made on coneless mice. For this, a flicker photometric procedure was used in which the response to a monochromatic test light flickering at 12.5 Hz was matched to that obtained from a similarly flickering interleaved reference light (Jacobs et al., 1996). Such measurements were made at 10-nm steps from 360 nm to 440 nm. The reference light was UV, produced by passing light through a bandpass filter (Schott UG11; transmission peak = 330 nm; half-bandwidth = 100 nm). Two complete wavelength scans were made and the photometric equations obtained from the two were subsequently averaged. Finally, amplitude versus response (V–log I) functions were obtained from coneless mice and wild-type controls. In making this measurement, the test eye was steadily exposed to a long-wavelength light produced by inserting a long-pass filter (50% transmission at 556 nm) in the adaptation beam of the optical system. This yielded 14.94 log photons/s/str (specified as weighted for their effectiveness on the mouse M pigment). This adaptation was sufficient to suppress completely any response to a 500-nm light in wild-type mice, thus presumably obviating any substantial contribution from mouse rods or M cones. The test light was UV; it was produced by placing a Schott UG1 filter having a transmission peak of 360 nm and a half-bandwidth of 60 nm in the path of the reference beam. The intensity of the test light was increased in successive steps of 0.2 and 0.3 log units from near threshold up to a level sufficient to produce response saturation. At each intensity step, mean response amplitudes were obtained from five stimulus trains each of which in turn consisted of 50 presentations of the test light (as described above). All of the ERG recordings were done in a room with ambient lighting that produced an illuminance of ~150 lux at the cornea of the test eye.

Photoreceptor labeling

Adult coneless mice and their wild-type littermates were euthanized by an overdose of halothane. Eyes were marked for orientation and enucleated. The cornea and lens were removed and the resulting eye cups were immersion fixed in 4% paraformaldehyde diluted in 0.086 M $NaPO_4$ buffer solution (pH 7.3).

Whole retinas were dissected from the eye cups and postfixed in 4% paraformaldehyde for 3 h. Next, the retinas were rinsed in phosphate buffered saline (PBS) and bathed overnight in either normal donkey serum or normal goat serum (1:20; Vector Labs, Burlingame, CA) diluted in a solution containing PBS, 0.1% Triton

X-100 (LabChem, Pittsburgh, PA), and 0.01% sodium azide (Sigma, St. Louis, MO), together referred to as PTA. Retinas were then incubated in a combination of biotinylated peanut agglutinin (PNA) lectin (1:1000 dilution; Vector Labs) to label cone matrix sheaths (Blanks & Johnson, 1984) and either JH492 antibody (Chiu et al., 1994), kindly provided by J. Nathans, or a goat polyclonal UV/S specific antibody (SC-14363; 1:1000 dilution; Santa Cruz Biotechnology, Santa Cruz, CA). After being rinsed with PTA, the retinas were then incubated for 24 h at 4°C in a combination of streptavidin conjugated to the fluorochrome Texas Red (Vector Labs; 1:200 dilution) and either a goat anti-rabbit secondary antibody conjugated to the CY2 fluorochrome (1:200 dilution; Jackson ImmunoResearch Laboratories, West Grove, PA) or a donkey anti-goat secondary antibody conjugated to the fluorochrome fluorescein (Vector Labs; 1:200 dilution). All antibodies were diluted in PTA. The retinas were rinsed in PTA then mounted on slides photoreceptor side up in fade-resistant mounting media (5% *n*-propyl gallate in glycerol). Control retinas were processed using only secondary antibodies. None of these demonstrated any photoreceptor labeling.

Digital images (0.031 mm^2) were collected at 1-mm intervals across each retina using a fluorescence microscope (Olympus BX-60) equipped with a CCD camera. The images were adjusted for brightness and contrast using Adobe Photoshop and labeled cells were counted manually. The average densities for each retina were used to estimate the total number cones as well as the number of cones containing each opsin class. For these estimates, we assumed the retina of the C57BL/6 mouse to have an area of 18.5 mm^2 (Zhou & Williams, 1999).

Behavioral tests

Visual sensitivity measurements were made in a three-alternative, forced-choice discrimination task. The apparatus and general procedures have been fully described previously (Jacobs et al., 1999, 2004). In brief, discrimination tests were conducted in a small test chamber in which lights were transprojected onto three test panels (2.5-cm diameter) that were arrayed in a line along one wall of the chamber where the center-to-center distance of the panels equaled 5 cm. These lights came from a 150-W tungsten-halide lamp and from an Instruments SA (H-10) grating monochromator (half-energy passband = 16 nm) equipped with a 75-W xenon lamp. The former light was used to diffusely, equally, and steadily illuminate the three panels. These served as background lights for increment-threshold measurements. Through an automated mirror system, monochromatic light was directed to any one of the three panels; this constituted the test light. The intensities of test and background lights were controlled through the use of a neutral-density wedge and neutral-density step filters, respectively.

Through an operant shaping procedure mice were trained to indicate the stimulus panel illuminated by the test light by touching it. Correct choices were reinforced by automated delivery of 0.028 ml of a highly palatable fluid (Soymilk, West Soy Plus Plain) from feeder tubes mounted above each of the stimulus panels. Over successive trials the location of the test light was randomly varied across the three panel positions. The nature of the difference between the test light and the background lights was systematically varied to make threshold measurements. Each test trial was indicated to the subject by concurrent presentation of the test light and a cueing tone, both of which terminated when the animal responded or after 15 s without a response. The intertrial duration was 6 s. In addition, a penalty time was assessed so that the onset of a test trial was delayed for 5 s following any between-trial responses. A noncorrection procedure was used, that is, an incorrect response was followed by a new trial the nature of which was as called for by the experimental protocol. In this test situation, mice typically completed 300–700 observations/test session. A variety of increment thresholds were measured; the stimulus details are given below.

Results

ERG signals from coneless and wild-type mice

It proved straightforward to distinguish coneless from wild-type animals with the flicker ERG. Wild-type mice gave clear responses to the achromatic test light (mean amplitude = 41 μV; n = 16; range: 14–50 μV) while coneless mice gave only small or inconsistent responses to this same test light (mean = 0.9 μV; n = 14; range: 0–10 μV). At the same time, this group of wild-type mice produced a robust response to the UV test light (mean = 127 μV; range: 79–170 μV) while the coneless mice gave much smaller, but still clear responses to the UV test (mean = 12.4 μV; range: 7–35 μV). These ERG classifications were verified by examining immunolabeled retinas. In each case, animals phenotyped by ERG recording as coneless were subsequently found to have retinas largely absent of cones.

The small but reliable ERG responses to a UV light recorded from putative coneless mice suggested that the small numbers of receptors containing UV pigment earlier observed to survive in such animals in fact contribute a significant input to the flicker ERG. To verify that, spectral sensitivity functions were measured for those animals believed to be coneless. Reliable spectral sensitivity functions were readily recorded from such animals for test wavelengths between 360 nm and 440 nm. The results are shown in Fig. 1 where the solid circles are mean values for 10 mice (±1 SD). Although it was not possible to make spectral sensitivity

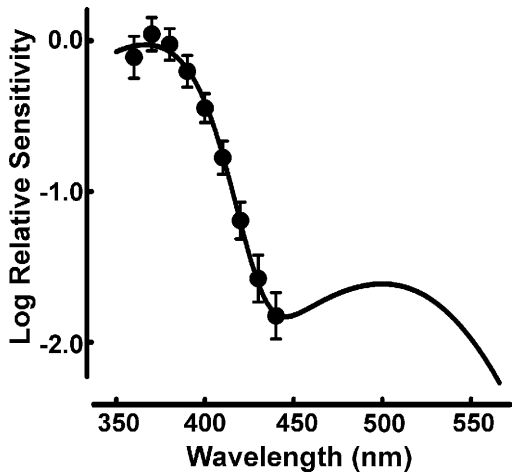

Fig. 1. Flicker-photometric ERG spectral sensitivity function derived for coneless mice. The solid circles are mean values (±1 SD) for ten animals. The sensitivity values were corrected for mouse lens absorption (unpublished measurements) and then best-fit with photopigment absorption curves (Govardovskii et al., 2000) as described in the text. The curve represents the linear summation of two photopigment absorption curves having respective peak values of 363 nm and 500 nm.

measurements for test lights longer than 440 nm, very small responses ($< 0.5\ \mu$V) could usually be elicited by a 500-nm test light. These responses presumably could reflect either residual contributions from rods to the 12.5-Hz flicker or signals from a small number of surviving M cones. Accordingly, to account for the spectral sensitivity function of Fig. 1, it was assumed that it reflected summative contributions from two mechanisms, one with a peak near that of mouse rods or M cones (roughly, 500 and 510 nm, respectively) and a second in the UV. The continuous line in Fig. 1 is that best-fit function with component contributions of 363 nm (98.8%) + 500 nm (1.2%). The fit is not substantially altered by changing the longer wavelength mechanism to a peak value appropriate for mouse M cones (i.e. with a peak of 510 nm), so it remains indeterminate as to which of the two contributes to the 12.5-Hz flicker ERG. In either case, the main signal contribution to the ERG has a spectral peak appropriate for mouse UV cone pigment (Jacobs et al., 1991; Yokoyama et al., 1998; Lyubarsky et al., 1999) and thus it seems evident that the small number of cones containing UV pigment can provide a significant input to the ERG in coneless mice.

The relative magnitude of the UV cone signal in the coneless mouse was evaluated by comparing V–log I functions for coneless and wild-type mice. The results are given in Fig. 2 where the solid circles and diamonds represent the respective mean amplitudes (± 1 SEM) recorded from wild-type ($n = 10$) and coneless ($n = 14$) mice. The continuous curves through the two data sets are least-squares fits derived from the hyperbolic equation: $V(I) = V_{max}[I^n/(I^n + K^n)]$, where K is the intensity required for a half-maximal response, n is the slope, and V_{max} is the saturation voltage (Fulton & Rushton, 1978). As can be appreciated by the inset to Fig. 2 where these functions are plotted in log/log coordinates, neither the K or n parameter values derived for the two types of mice were significantly different (independent samples t-tests: for K, $t(23) = -0.94323$, $P = 0.356$, two-tailed; for n: $t(23) = 2.54$, $P = 0.013$, two-tailed). The V_{max} values for the two groups were, obviously, greatly different from those of wild-type mice ($M = 158.6\ \mu$V) being on average about ten times greater than the value similarly derived for coneless animals (16.2 μV; t (23) = 12.696. $P < 0.001$, one-tailed). Although the V_{max} values for coneless mice were very much smaller than for wild-type animals, there was some obvious variation in the voltages recorded among the individual coneless mice. The significance of that observation is addressed below.

Photoreceptor labeling

Fig. 3 illustrates photoreceptor labeling obtained for the three markers in representative sections taken from the retinas of wild-type and coneless mice. As estimated by PNA labeling, the retinas of wild-type mice contained on average a total of 189,303 cones (SD = 7230, $n = 5$). This value is similar to that of earlier counts made on wild-type C57BL/6 mice (Jeon et al., 1998). PNA counts made on retinas from coneless mice show a drastic reduction in the total cone population (mean = 7074; SD = 3400; $n = 13$; $t(16) = 74.27$, $P < 0.001$, one-tailed). The size of the residual cone population, being ~4% of that of the wild-type, is in line with

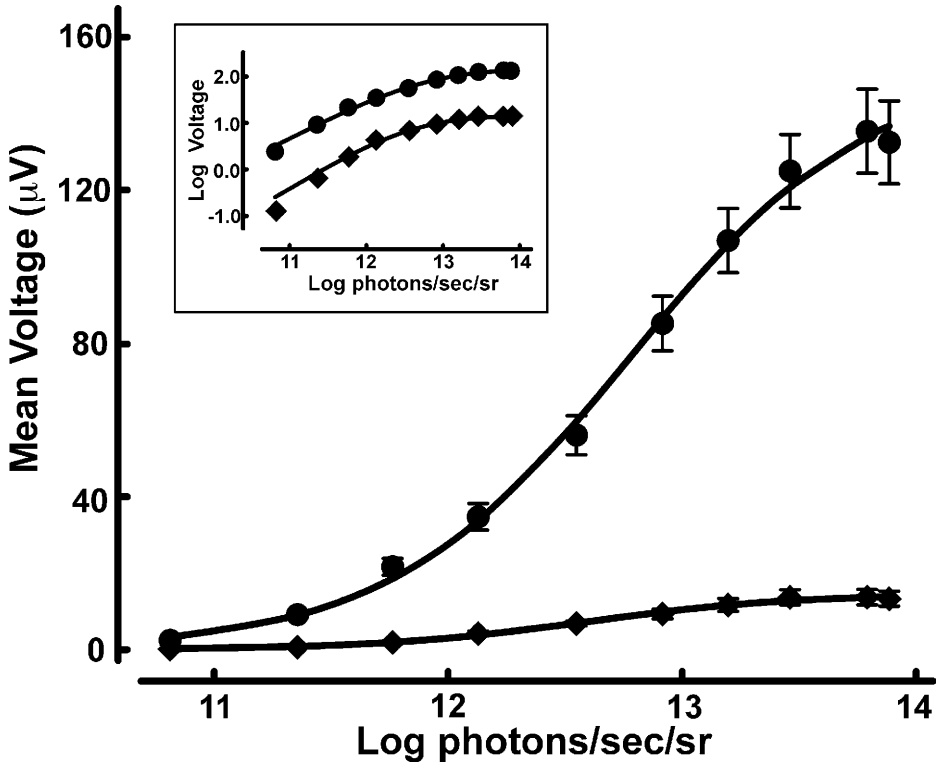

Fig. 2. ERG intensity response (V–log I) functions for the isolated UV cone signals recorded in wild-type and coneless mice. The data plotted are mean amplitudes (± 1 SEM) recorded to each of the test intensities. Results are shown for 11 wild-type mice (circles) and 14 coneless mice (diamonds). The lines represent best least-squares fits derived as described in the text. The inset shows the same data set as rendered in log/log coordinates. The intensities of the test lights were specified by weighting the UV stimulus according to its effectiveness on the mouse UV photopigment.

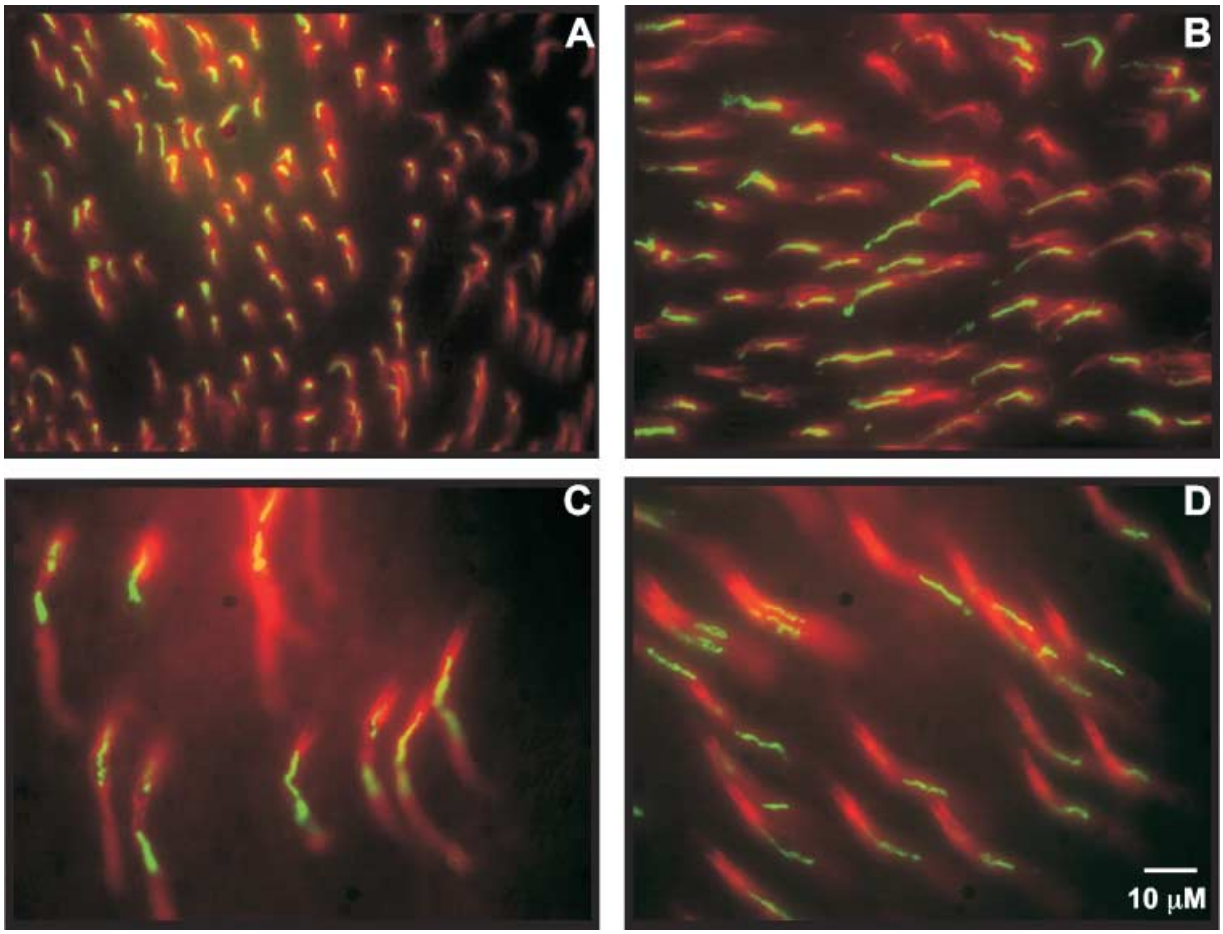

Fig. 3. Labeled cones in the retinas of wild-type (top panels) and coneless (bottom panels) mice. Panels A and C: Cones labeled with a combination of PNA and M opsin specific antibody. Panels B and D: Cones labeled with a combination of PNA and UV opsin specific antibody. The scale bar in the lower right panel is appropriate for all panels.

other estimates for similarly derived coneless mice (Soucy et al., 1998; Raven & Reese, 2003).

The two types of mouse cone pigment may be co-expressed in single cones (Rohlich et al., 1994). Estimates of the extent of this co-expression and of its regional patterning across the retina vary somewhat, but recent studies agree that it is quite extensive (Glosmann & Ahnelt, 1998; Applebury et al., 2000). A consequence is that the two opsin immunolabels may frequently identify the same cones. In retinas from two wild-type mice an average of ~72% of the total cones were labeled with the M-cone opsin antibody, while in retinas from three wild-type mice ~53% of the total cones were labeled with the UV/S-cone opsin antibody. In confirmation of previous results, a vast majority (~87%) of the receptors surviving in the coneless retina contained UV opsin; eight retinas probed for the presence of UV opsin contained a mean of 6146 cones (SD = 2994). Cones containing M-pigment in the coneless retina were sparse; retinas examined with the M-cone opsin antibody yielded on average a total of only 744 cones (SD = 79; $n = 5$). Although we made no formal analysis of the retinal distribution of the surviving cones, a majority of the cones containing UV pigment appear to be in the ventral retina while the few remaining M cones were scattered across the retina. Both of these observations are in line with previous reports (Soucy et al., 1998; Raven & Reese, 2003).

Visual sensitivity in wild-type and coneless mice

Five mice (two wild-type, three coneless) were trained to make visual discriminations. There were no obvious differences between the two types of mice either in the amount of training required to learn the task or in their eventual accuracy. Over a period of about 8 months increment thresholds were measured under a variety of test conditions for each of these animals. The background lights for all threshold measurements were achromatic (5350 K). A number of different test lights were used; most of the measurements reported here were for a test light of 500 nm. Thresholds were first measured with dim background lights and over time these threshold measurements were extended to include progressively brighter backgrounds such that, in total, the range of background light levels extended from −1.37 to 2.37 log scot. cd/m^2. The lowest background light level tested is approximately four log units above the value obtained as a measure of absolute visual threshold for a pulsed stimulus light in C57BL/6 mice (Herreros de Tejada et al., 1997).

With low levels of light adaptation, the visual sensitivity of coneless mice was indistinguishable from that of similarly tested control animals. This fact is illustrated in Fig. 4 which shows psychometric functions derived for detection of two monochromatic test lights (500 nm and 600 nm) added to a dim (−1.37 log

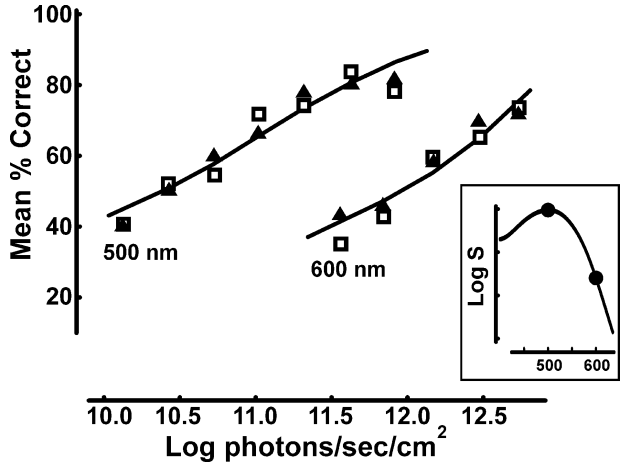

Fig. 4. Mean psychometric functions obtained from two wild-type mice (squares) and three coneless mice (triangles) in a increment-threshold discrimination task. The data reflect the performance cumulated over a total of 100 trials per animal at each of the test light intensities. These results were then averaged across the animals in each group. Background light: achromatic, − 1.4 log scot. cd/m^2; test lights: 500 nm (left), 600 nm (right). The performance data were best-fit to logistic functions having asymptotes of 100 and 33% correct with the variance and mean values as free parameters. The inset shows the two-point spectral sensitivity function derived for these two test lights. The spectral peak of the photopigment absorption curve that best fits these data is 500.3 nm.

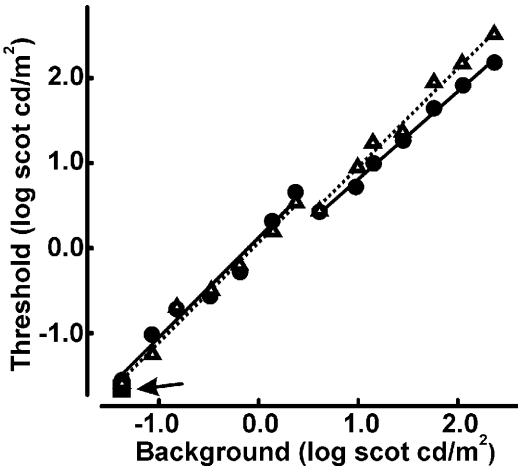

Fig. 5. Mean increment-threshold functions for wild-type (circles, $n = 2$) and coneless (triangles, $n = 3$) mice. The background light was achromatic; the test light was 500 nm. Each data point was derived from performance data for each animal similar in nature to those illustrated in Fig. 4. Linear regressions were fit to the two segments of the threshold functions for both types of mice. For the dimmer background light levels ($< \sim$0.4 log scot. cd/m^2) the functions are not significantly different. Across the brighter background light levels ($\gtrsim$1 log scot. cd/m^2) the slopes are significantly different [$t(10) = 1.86$, $P < 0.05$]. An increment threshold was remeasured for one coneless mouse at 21 months of age. That threshold value is indicated by the arrow at the bottom left.

scot. cd/m^2) background. As can be seen, the mean % correct detection is indistinguishable for the two types of mice across a test light intensity range sufficient to produce discrimination performance from near chance up to about 80% correct. These results can be used in the standard fashion to infer the nature of the photopigment underlying this behavior. The photopigment absorption function that provided the best least-squares fit to these two spectral points (inset to Fig. 4) has a peak of 500.3 nm. That spectral location is very close to that established for the mouse rod pigment (Lyubarsky et al., 1999) and so we conclude that under low-level light adaptation both coneless and wild-type mice possess equally effective rod-based vision.

Increment thresholds were measured using a 500-nm test light on a total of 15 backgrounds varying in luminance upwards from that of Fig. 4. In each case, thresholds were defined as the test intensities required to support performance at the upper 99% confidence interval. The results are summarized in Fig. 5 which plots the mean thresholds obtained from two wild-type and three coneless mice as a function of luminance of the background light. From ~ -1.37 log scot. cd/m^2 up to $\sim$ 0.40 log scot. cd/m^2, the threshold values for coneless and wild-type mice are virtually identical. Linear regressions fit to the two data sets yield slopes of 1.172 and 1.176, respectively. None of the mice showed an increase in threshold at the next background light level (0.61 log scot. cd/m^2), in fact both showed a slight decrease, but above that value thresholds again rose systematically as a function of background luminance. For background luminance values $> \sim$1 log scot. cd/m^2, thresholds obtained from the coneless mice rose more rapidly than did those for wild-type mice. The result is that the line fit to the coneless data has a significantly steeper slope (1.16 *vs.* 1.03) across the higher luminances than does the line similarly fit to data from the control animals [$t(10) = 1.86$, $P < 0.05$]. It is noteworthy that at the highest background light level where it was possible to derive threshold measurements (2.37 log scot. cd/m^2) the coneless mice continued to still show little difficulty in making visual discriminations.

To identify the receptors that underlie visual performance at the higher levels of light adaptation, we measured complete spectral sensitivity functions for two animals—one coneless and one wild-type. Optical system limitations were such that the brightest adaptation level on which it was possible to measure a full spectral sensitivity function corresponded to a panel luminance of 1.76 log scot. cd/m^2. The resulting spectral sensitivity functions are shown in Fig. 6. To identify the spectral mechanisms underlying this behavior, we first searched for the photopigment absorption function that provided the best fit to the spectral sensitivity function for all wavelengths longer than 480 nm. The logic behind this procedure is that the mouse UV pigment has very low sensitivity over this part of the spectrum and thus this fit should characterize only the longer spectral mechanisms in the mouse (i.e. rod pigment and M cone). The spectral mechanisms so identified had peak values of 500.2 and 508.3 for the coneless and wild-type mice, respectively, implying that sensitivity over the middle to long wavelengths reflects contributions from different receptor types, rods for the coneless animal, and M cones for the wild-type mouse. Next, we set the long-wavelength component to have these two peak values and asked whether a curve then fit to the entire data array for each animal could be improved by linearly adding contributions from a second spectral mechanism with a peak value found (above) to characterize the mouse UV cone. In the case of the wild-type mouse, the full function was best fit by linearly summing standard photopigment absorption curves having respective peak values of 508.3 and 363 nm with relative proportions of 85.7% and 14.3%. The fit to the data array for the coneless animal is optimized for

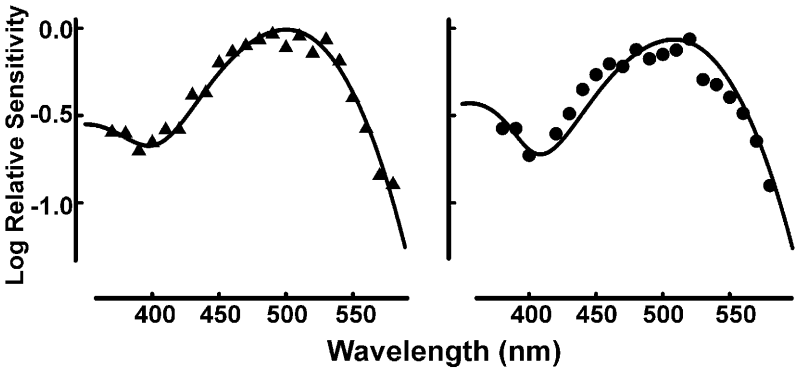

Fig. 6. Increment-threshold spectral sensitivity functions obtained from a coneless (left panel) and a wild-type mouse (right panel). The background luminance was 1.76 log scot. cd/m^2. The spectral sensitivity functions have each been fit to linear summations of two photopigment absorption functions as described in detail in the text.

pigments having respective peaks of 500.2 and 363 nm, the two linearly summed in proportions of 98% and 2%, respectively.

Discussion

Cone-specific expression of an attenuated diphtheria toxin largely kills off the cone population in the retina of a developing mouse. Yet in these so-called coneless animals some cones do survive (~4% of the normal complement). These surviving cones predominantly contain UV pigment and, although they are few in numbers, their presence can be readily detected in the corneally recorded ERG. Observations made on these coneless mice have implications both for their use as an animal model and, more generally, for circumstances where photoreceptor populations are greatly reduced by disease or experimental manipulation.

Rod function in coneless mice

Loss of one receptor type as a result of disease often triggers a subsequent loss of the other type. Thus, for example, rod loss in the rd/rd mouse leads secondarily to cone cell loss (Jimenez et al., 1996), and in the case of retinitis pigmentosa rod cell death is followed by cone death (Dryja & Li, 1995). This linkage is not, however, inevitable. In a much studied form of inherited color blindness, complete achromatopsia, cone function is entirely absent yet most measures indicate the presence of normal or even superior rod-based vision (Hess et al., 1987; Skottun et al., 1981). This variation seems to be paralleled in four different coneless mouse models. As noted above, the transgenic mouse that is the subject of this investigation was earlier reported to have normal rod signals as evidenced by recordings made from ganglion cells (Soucy et al., 1998) and, similarly, a coneless mouse produced by genetically deleting a cyclic nucleotide-gated channel (CNG3) and a transgenic mouse in which degeneration was induced by cone-specific expression of an onocogene (*Mas 1*) were found to have normal rod ERGs (Soucy et al., 1998; Biel et al., 1999; Xu et al., 2000). On the other hand, coneless mice produced by expressing an attenuated diphtheria toxin but with different promoter and enhancer elements than those used here have a profound age-related rod loss; indeed, in such mice the entire outer retina had degenerated by only a few months of age (Ying et al., 2000). Why cone loss leads to rod degeneration in some cases but not others is uncertain, but differences in the techniques used to destroy cones may be key, perhaps related to the developmental timing of cone cell death.

For those coneless mice that retain rods, the functioning of the rod system was earlier evidenced by measurements of ERG amplitudes and ganglion cell firing rates (Soucy et al., 1998; Biel et al., 1999). While both of these retinal measures argue that early stages of the rod system are at least near normal, a potentially more compelling index of rod function can be obtained from measurements of visual sensitivity which index the entire rod-based visual system. Threshold measurements made at low light levels (Fig. 4) show that coneless mice and their normal littermates have essentially identical visual sensitivity and thus coneless mice must have a rod system that operates normally. Our measurements further suggest that the normality of the rod system in the coneless mouse is not age limited. The behavioral measurements were made on coneless mice over a time period extending from about 3 to 11 months of age. No deterioration in performance was seen across this time span. To assess whether there still might be long-term degeneration of the rod system in the coneless mouse, one of these mice was returned to the behavioral task nearly a year after completing the original measurements. At that point an additional rod threshold was measured following the same test protocol as that described above. That new threshold value is plotted in Fig. 5 (indicated by the arrow at the lower left). Clearly, even at 21 months of age the rod system of the coneless mouse shows no functional evidence of deterioration.

At moderate to intermediate light levels mammalian rods saturate. For human observers rod saturation occurs at luminances falling in the range from 1.94 to 3.3 log cd/m^2 (Makous, 2004). On the most intense background where it was still possible to measure increment thresholds in coneless mice (a panel luminance of 2.37 log scot.cd/m^2) there was no evidence of rod saturation. To assess whether rod saturation in the mouse would be expected under these conditions, we assumed that the behavioral viewing circumstance essentially provided ganzfeld stimulation and that pupil size was controlled by panel luminance in accord with the relationship between illumination and pupil size earlier established for C57BL/6 mice (Pennesi et al., 1998). With those assumptions, and following the relationships derived by Lyubarsky and colleagues (Lyubarsky et al., 2004), this implies this background light should yield $\sim 3.2 \times 10^3$ photoisomerizations/rod/s. This is considerably less than the 4–5 log photoisomerizations/rod/s earlier shown to be required to completely abolish the rod-driven ganglion cell response in coneless mice (Soucy et al., 1998), and thus these background light levels are well short of those that would be required to saturate the mouse rod system. Part of the failure to achieve rod saturation seems traceable to the fact that the size of the mouse pupil constricts over a large range and thus serves rather

effectively to keep retinal illumination below the levels required for rod saturation (Pennesi et al., 1998). An implication of this is that many laboratory studies of mice done with natural viewing are unlikely to achieve the light levels necessary to completely obviate rod signals. Comparison of the thresholds measured for coneless and control animals further suggests that for a test light set close to both their respective sensitivity peaks, behavioral rod threshold begins to exceed that for the cones when rod photoisomerization rates reach ~110/rod/s.

Cone function in coneless mice

The failure to detect cone-related signals in the earlier study of coneless mice (Soucy et al., 1998) seems likely to have been due to the absence of sufficient light from that part of the spectrum to which mouse UV cones are most sensitive. Although in the present study UV stimulation yielded consistently reliable ERG signals in coneless mice, these same animals were largely unresponsive to an "achromatic" test light. These facts underline the view that in assessing the effects of treatments that alter retinal function in mice it is important to employ stimuli appropriate to activating UV as well as M cones.

A recent study using cone-isolating stimuli concluded that the amplitude of the ERG recorded from the human eye is proportional to the number of cones being stimulated (Murray et al., 2004). The test conditions used to obtain V–log I functions (Fig. 2) effectively isolate signals from mouse cones that contain UV pigment. Since the number of cones surviving in coneless mice varies from animal to animal, these animals allow the possibility of directly examining the relationship between ERG amplitude and the size of the cone complement. Fig. 7 shows the relationship between the V_{max} values obtained from ERG measurements made on seven coneless mice and the total number of UV cones their retinas contained. There is a significant positive correlation between ERG amplitude recorded at response saturation and the estimated number of UV cones such that, at least over the range of numbers of receptors represented in Fig. 7, there is linear relationship between cone number and ERG voltage. Even the retina with the lowest number of surviving UV cones (~3600) produced a V_{max} value of about 5 μV. The recording arrangement employed permits very reliable recording of signals having average amplitudes of ~1 μV. If the relationship between cone number and voltage graphed in Fig. 7 continues to hold for still smaller values, this would imply that it should be possible to reliably record ERG signals from a mouse retina having a total cone population of something just over 2000 receptors. If the same relationship holds for mouse M cones, this result would further imply that the residual M cone population in the coneless mouse, averaging as it does fewer than 800 receptors, would be unlikely to generate signals that could be detected with the present ERG setup.

The survival of cones containing UV pigment in the coneless mouse was earlier suggested to be due to the fact that the human L-cone opsin gene promoter activity is lower in mouse UV cones than in M cones thus accounting for the variegated expression of the diphtheria toxin gene (Soucy et al., 1998). Fig. 8 plots the relationship between the numbers of surviving cones containing the two types of pigment relative to the total numbers of cones found in coneless mice. It is apparent that in these animals the total number of surviving M cones is independent of the total number of cones while UV cone survival increases proportionally with total cones. This relationship provides support for the claim of Soucy and colleagues (Soucy et al., 1998) that it is the variable influence of the opsin gene promoter on UV cones that accounts for the partial survival of these cones in the coneless mouse. If that is the case, it might also be expected that the degree of cone survival would be more similar in the two eyes of an individual mouse than it is across individuals. Total cone counts were made in both retinas of six coneless mice. The average difference in the number of surviving cones in the two eyes taken from the same animal were found to be significantly lower than the average difference between all pairs of eyes in the sample [$t(5) = 6.058$, $P = 0.002$].

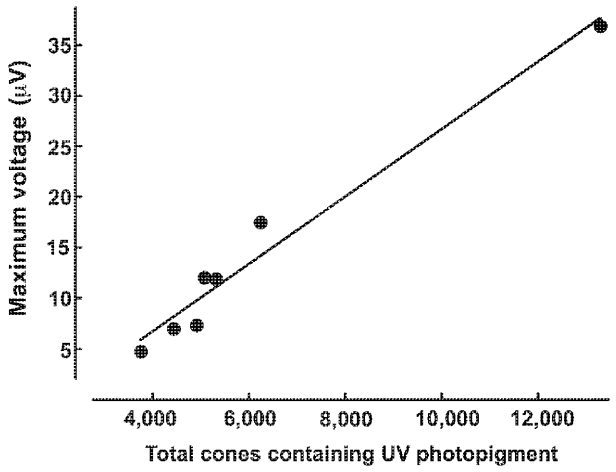

Fig. 7. Relationship between the total number of cones containing UV photopigment found in the retinas of seven coneless mice and the maximum voltage recorded from each animal in ERG measurements. The V_{max} values were obtained for each animal under test conditions that effectively isolate signals from UV cones. The line represents the best linear fit to the data. There is a significant positive correlation between the two measures ($r^2 = 0.967$, $P < 0.0001$).

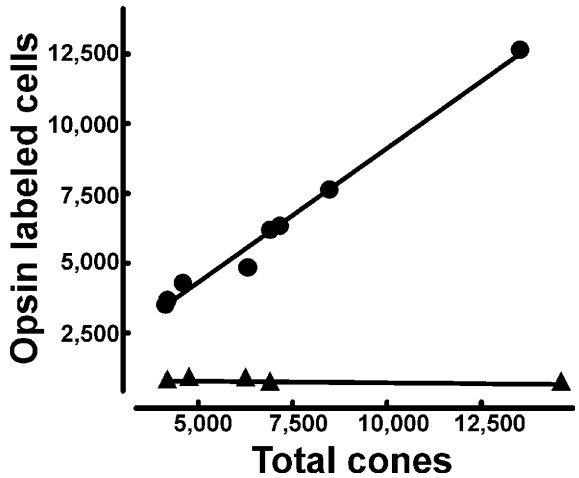

Fig. 8. The relationship between the total numbers of cones estimated in the retinas of coneless mice and the number of cones containing UV (circles) and M (triangles) cone pigment in retinas double labeled with PNA and either M or UV opsin specific antibodies. A linear regression has been determined for each pigment type. The number of cones containing M pigment is independent of the total cone count ($r^2 = 0.385$) whereas UV cone survival increases proportionally with the total number of cones ($r^2 = 0.989$, $P < 0.0001$).

This suggests that the factors limiting cone survival in this model are not local to individual retinas.

Although it was straightforward to detect signals originating from cones containing UV pigment in the coneless mouse, it is less clear that these can be used to guide visual behavior. There is a hint of a small contribution from a UV mechanism to the increment-threshold spectral sensitivity function of the coneless mouse measured with a moderately bright background (Fig. 4), but its presence is admittedly somewhat arguable. Although we believe it likely that the residual UV signal in these coneless mice can indeed support some visual behaviors, it was not possible to arrange viewing circumstances favorable enough to demonstrate its clear emergence in the current test situation.

Coneless mice as models

We have shown that the residual cones in the retina of the coneless mouse contribute significantly to retinal signals and that, potentially, these may then allow cone-based influence on the organization of the visual system and on behavior. If the goal of a research project requires a complete absence of cone influence, then this transgenic mouse is not adequate. For many purposes, however, this mouse can provide a useful model of a visual system that is effectively absent cone influence. For instance, it would be relatively easy to arrange photic rearing conditions or stimulus test conditions that would not stimulate the handful of surviving UV cones. Beyond that, this animal also offers advantages. One of these is that other than a direct reduction in the number of cones, there is no obvious gross degeneration of the retina. This sets this animal model apart from other manipulations that reduce the receptor complement but then also trigger significant degeneration changes in the retina. Finally, there are numerous retinal diseases as well as experimental treatments that reduce but do not fully remove the receptor complement. Those cases have oftentimes revealed a surprising retention of visual function in the face of massive receptor loss; for example, significant losses of cones in Stargardt's disease are associated with quite modest declines in visual acuity (Geller & Sieving, 1993) and only a handful of photoreceptors surviving in the retinas of light-damaged rats are sufficient to support rudimentary visual discriminations (Anderson & O'Steen, 1972; Williams et al., 1985). The coneless mouse provides a clear opportunity to study more searchingly the retention of visual function in an animal that has suffered a near complete loss of a single photoreceptor type.

Acknowledgments

We thank Ben Reese and Mary Raven for providing animals and John Fenwick for help with the anatomy. This research was supported by a grant from the National Eye Institute (EY002052).

References

Alpern, M., Lee, G.B., Maaseidvaag, F. & Miller, S.S. (1971). Colour vision in blue-cone monochromacy. *Journal of Physiology* **212**, 211–233.

Anderson, K.V. & O'Steen, W.K. (1972). Black-white and pattern discriminations in rats without photoreceptors. *Experimental Neurology* **34**, 446–454.

Applebury, M.L., Antoch, M.P., Baxter, L.C., Chun, L.L.Y., Falk, J.D., Farhangfar, F., Kage, K., Kryzystolik, M.L., Lyass, L.A. & Robbins, J.T. (2000). The murine cone photoreceptor: A single cone type expresses both S and M opsins with retinal spatial patterning. *Neuron* **27**, 513–523.

Biel, M., Seeliger, M., Pfeifer, A., Kohler, K., Gerstiner, A., Ludwig, A., Jaissle, G., Fauser, S., Zrenner, E. & Hofman, F. (1999). Selective loss of cone function in mice lacking the cyclic nucleotide-gated channel CNG3. *Proceedings of the National Academy of Sciences of the U.S.A.* **96**, 7553–7557.

Blanks, J. & Johnson, L.V. (1984). Specific binding of peanut lectin to a class of retinal photoreceptor cells: A species comparison. *Investigative Ophthalmology and Visual Science* **25**, 546–557.

Buck, S.L. (2004). Rod-cone interactions in human vision. In *The Visual Neurosciences, Vol. 1*, ed. Chalupa, L.M. & Werner, J.S., pp. 863–878. Cambridge, Massachusetts: MIT Press.

Carter-Dawson, L.D., LaVail, M.M. & Sidman, R.L. (1978). Differential effects of the rd mutation on rods and cones in the mouse retina. *Investigative Ophthalmology and Visual Science* **17**, 489–498.

Chiu, M.I., Zack, D.J., Wang, Y. & Nathans, J. (1994). Murine and bovine blue cone pigment genes: Cloning and characterization of the S family of visual pigments. *Genomics* **21**, 440–443.

Dang, L., Pulukuri, S., Mears, A.J., Swaroop, A., Reese, B.E. & Sitaramayya, A. (2004). Connexin 36 in photoreceptor cells: Studies on transgenic rod-less and cone-less mouse retinas. *Molecular Vision* **10**, 323–327.

Dryja, T.P. & Li, T. (1995). Molecular genetics of retinitis pigmentosa. *Human Molecular Genetics* **4**, 1739–1743.

Fulton, A.B. & Rushton, W.A.H. (1978). The human rod ERG: Correlation with psychophysical responses in light and dark adaptation. *Vision Research* **18**, 793–800.

Geller, A.M. & Sieving, P.A. (1993). Assessment of foveal cone photoreceptors in Stargardt's macular dystrophy using a small dot detection task. *Vision Research* **33**, 1509–1524.

Glosmann, M. & Ahnelt, P.K. (1998). Coexpression of M- and S-opsin extends over the entire inferior mouse retina. *Investigative Ophthalmology and Visual Science* **39**, S1059.

Govardovskii, V.I., Fyhrquist, N., Reuter, T., Kuzmin, D.G. & Donner, K. (2000). In search of the visual pigment template. *Visual Neuroscience* **17**, 509–528.

Herreros de Tejada, P., Munoz Tedo, C. & Costi, C. (1997). Behavioral estimates of absolute visual threshold in mice. *Vision Research* **37**, 2427–2432.

Hess, R.F., Nordby, K. & Pointer, J.S. (1987). Regional variation of contrast sensitivity across the retina of the achromat: Sensitivity of human rod vision. *Journal of Physiology* **388**, 101–119.

Jacobs, G.H. (1993). The distribution and nature of colour vision among the mammals. *Biological Reviews* **68**, 413–471.

Jacobs, G.H., Fenwick, J.C., Calderone, J.B. & Deeb, S.S. (1999). Human cone pigment expressed in transgenic mice yields altered vision. *Journal of Neuroscience* **19**, 3258–3265.

Jacobs, G.H., Neitz, J. & Deegan, II, J.F. (1991). Retinal receptors in rodents maximally sensitive to ultraviolet light. *Nature* **353**, 655–656.

Jacobs, G.H., Neitz, J. & Krogh, K. (1996). Electroretinogram flicker photometry and its applications. *Journal of the Optical Society of America A* **13**, 641–648.

Jacobs, G.H., Williams, G.A. & Fenwick, J.A. (2004). Influence of cone pigment coexpression on spectral sensitivity and color vision in the mouse. *Vision Research* **44**, 1615–1622.

Jeon, C.-J., Strettoi, E. & Masland, R.H. (1998). The major cell populations of the mouse retina. *Journal of Neuroscience* **18**, 8936–8946.

Jimenez, A.J., Garcia-Fernandez, J.-M., Gonzalez, B. & Foster, R.G. (1996). The spatio-temporal pattern of photoreceptor degeneration in the aged rd/rd mouse retina. *Cell and Tissue Research* **284**, 193–202.

Lucas, R.J., Freedman, M.S., Munoz, M., Garcia-Fernandez, J.-M. & Foster, R.G. (1999). Regulation of the mammalian pineal by non-rod, non-cone ocular photoreceptors. *Science* **284**, 505–507.

Lyubarsky, A.L., Daniele, L.L. & Pugh, E.N.J. (2004). From candelas to photoisomerizations in the mouse eye by rhodopsin bleaching *in situ* and the light-rearing dependence of the major components of the mouse ERG. *Vision Research* **44**, 3235–3251.

Lyubarsky, A.L., Falsini, B., Pennesi, M.E., Valentini, P. & Pugh, Jr., E.N. (1999). UV- and midwave-sensitive cone-driven retinal responses of the mouse: A phenotype for coexpression of cone photopigments. *Journal of Neuroscience* **19**, 442–455.

Makous, W. (2004). Scotopic vision. In *The Visual Neurosciences, Vol. 1*, ed. Chalupa, L.M. & Werner, J.S., pp. 838–850. Cambridge, Massachusetts: MIT Press.

Murray, I.J., Parry, N.R.A., Kremers, J., Stepien, M. & Schild, A. (2004). Photoreceptor topography and cone-specific electroretinograms. *Visual Neuroscience* **21**, 231–235.

Pennesi, M.E., Lyubarsky, A.L. & Pugh, E.N.J. (1998). Extreme responsiveness of the pupil of the dark-adapted mouse to steady retinal illumination. *Investigative Ophthalmology and Visual Science* **39**, 2148–2156.

Raven, M.A. & Reese, B.E. (2003). Mosaic regularity of horizontal cells in the mouse retina is independent of cone photoreceptor input. *Investigative Ophthalmology and Visual Science* **44**, 965–973.

Reese, B.E., Raven, M.A. & Stagg, S.B. (2005). Afferents and homotypic neighbors regulate horizontal cell morphology, connectivity, and retinal coverage. *Journal of Neuroscience* **25**, 2167–2175.

Rohlich, P., van Veen, T. & Szel, A. (1994). Two different visual pigments in one retinal cone cell. *Neuron* **13**, 1159–1166.

Saugstad, P. & Saugstad, A. (1959). The duplicity theory. In *Advances in Ophthalmology, Vol. 9*. ed. Streif, D.B., pp. 1–51. Basel, Karger.

Skottun, B.C., Nordby, K. & Magnussen, S. (1981). Photopic and scotopic flicker sensitivity of a rod monochromat. *Investigative Ophthalmology and Visual Science* **21**, 877–879.

Sokal, I., Hu, G., Liang, Y., Mao, M., Wensel, T.G. & Palczewski, K. (2003). Identification of portein kinase C isozymes responsible for the phophorylation of photoreceptor-specific RGS9-1 at Ser475. *Journal of Biological Chemistry* **278**, 8316–8325.

Soucy, E., Wang, Y., Nirenberg, S., Nathans, J. & Meister, M. (1998). A novel signalling pathway from rod photorceptors to ganglion cells in mammalian retina. *Neuron* **21**, 481–493.

Sterling, P. (2004). How retinal circuits optimize the transfer of visual information. In *The Visual Neurosciences, Vol. 1*. ed. Chalupa, L.M. & Werner, J.S., pp. 234–259. Boston, Massachusetts: MIT Press.

Williams, R.A., Pollitz, C.H., Smith, J.C. & Williams, T.P. (1985). Flicker detection in the albino rat following light-induced retina damage. *Physiology and Behavior* **34**, 259–266.

Xu, X., Quiambao, A.B., Roveri, L., Pardue, M.T., Marx, J.L., Rohlich, P., Peachy, N.S., & Al-Ubaidi, M.R. (2000). Degeneration of cone photoreceptors induced by expression of the Mas 1 protooncogene. *Experimental Neurology* **163**, 207–219.

Ying, S., Jansen, H.T., Lehman, M.N., Fong, S.-L. & Kao, W.W.Y. (2000). Retinal degeneration in cone photoreceptor cell-ablated transgenic mice. *Molecular Vision* **6**, 101–108.

Yokoyama, S., Radlwimmer, F.B. & Kawamura, S. (1998). Regeneration of ultraviolet pigments of vertebrates. *FEBS Letters* **423**, 155–158.

Zhou, G. & Williams, R.W. (1999). Mouse models for myopia: An analysis of variation in eye size in adult mice. *Optometry and Vision Science* **76**, 408–418.